Carbon Nanotube Core Graphitic Shell Hybrid Fibers

Myung Gwan Hahm,[†,*] Jae-Hwang Lee,[‡] Amelia H. C. Hart,[‡] Sung Moo Song,[§] Jaewook Nam,[⊥] Hyun Young Jung,[∥] Daniel Paul Hashim,[‡] Bo Li,[‡] Tharangattu N. Narayanan,[‡] Chi-Dong Park,[#] Yao Zhao,[‡] Robert Vajtai,[‡] Yoong Ahm Kim,[△] Takuya Hayashi,[▽] Bon-Cheol Ku,[○] Morinobu Endo,[#] Enrique Barrera,[‡] Yung Joon Jung,[∥] Edwin L. Thomas,[‡] and Pulickel M. Ajayan[‡,*]

[†]Advanced Functional Thin Films Department, Surface Technology Division, Korea Institute of Materials Science, 797 Changwondaero, Sungsan-Gu, Changwon, Gyeongnam 642-831, Korea, [‡]Department of Mechanical Engineering and Materials Science, Rice University, Houston, Texas 77005, United States, [§]Department of Mechanical System Engineering, Shinshu University, Faculty of Engineering, 4-17-1 Wakasato, Nagano, 380-8553, Japan, [⊥]School of Chemical Engineering, Sungkyunkwan University, 300 Cheongcheon-dong, Suwon, Gyeonggi-do, 440-746, Korea, [∥]Mechanical and Industrial Engineering, Northeastern University, Boston, Massachusetts 02115, United States, [#]Research Center for Exotic Nanocarbons, Faculty of Engineering, Shinshu University, 4-17-1 Wakasato, Nagano, 380-8553, Japan, [△]Polymer & Fiber System Engineering, Chonnam National University, 77 Yongbong-ro, Buk-gu, Gwangju, 500-757, Korea, [▽]Faculty of Engineering, Shinshu University, 4-17-1 Wakasato, Nagano, 380-8553, Japan, and [○]Carbon Convergence Materials Research Center, Institute of Advanced Composites Materials, Korea Institute of Science and Technology, Eunhari san 101, Wanju-gun, Jeollabuk-do, 565-902, Korea

ABSTRACT A carbon nanotube yarn core graphitic shell hybrid fiber was fabricated *via* facile heat treatment of epoxy-based negative photoresist (SU-8) on carbon nanotube yarn. The effective encapsulation of carbon nanotube yarn in carbon fiber and a glassy carbon outer shell determines their physical properties. The higher electrical conductivity (than carbon fiber) of the carbon nanotube yarn overcomes the drawbacks of carbon fiber/glassy carbon, and the better properties (than carbon nanotubes) of the carbon fiber/glassy carbon make up for the lower thermal and mechanical properties of the carbon nanotube yarn *via* synergistic hybridization without any chemical doping and additional processes.

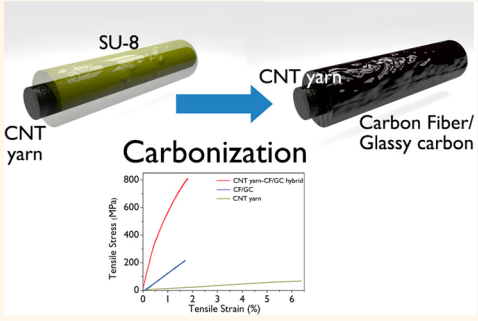

KEYWORDS: carbon nanotube yarn · carbon fiber · hybrid fiber · tensile strength · electrical conductivity · thermal conductivity

During the last few decades, there have been great advances in nanotechnology that can be used to create diverse state-of-the-art materials.[1−4] Obviously, carbon-based nanomaterials are one of the major driving forces in these developments.[5−9] Carbon nanotubes (CNTs), in particular, have attracted significant interest for industrial applications, due to their outstanding physical properties (mechanical strength, high electrical and thermal conductivities).[10] The remarkable physical properties of individual CNTs can be translated into a wide range of nanoscaled applications including, but not limited to, flexible nanoelectronics, chemical and mechanical sensing, multifunctional membranes, supercapacitors, and nanocomposites.[6,9,11−19] However, utilizing CNTs in many macroscale devices is limited by the difficulties in controlling the physical dimensions of CNT structures, especially length. The problems with synthesizing and then controlling the assembly of longer CNT structures has led to the use of alternative approaches, for example, combining shorter CNTs into longer structures, such as developing CNT yarn using dry/wet spinning techniques.[20−25] Yarns generated from CNTs possess unique intrinsic properties due to the parallel alignment of the CNTs in the tangential axis of the yarn and inherent physical properties of the CNTs.[20,22−24] The enhanced performance of the CNT yarns or fiber should be a key factor in enabling the utilization of CNTs in macroscale applications. However, despite this potential there is a huge chasm between theoretical and experimentally measured properties due to the defects in CNT material and inhomogeneities originating from the spinning process.[26] Various post-treatments including twisting, densification, and cross-linking have been attempted in order to alleviate these problems, but have not yet been sufficient to enable CNT yarn/fiber to be used for macroscale applications.[6,27−31]

Here, we report the development of a hybrid CNT yarn encapsulated in a carbon

* Address correspondence to mghahm@kims.re.kr; ajayan@rice.edu.

Received for review August 30, 2013 and accepted November 6, 2013.

Published online November 13, 2013
10.1021/nn4045276

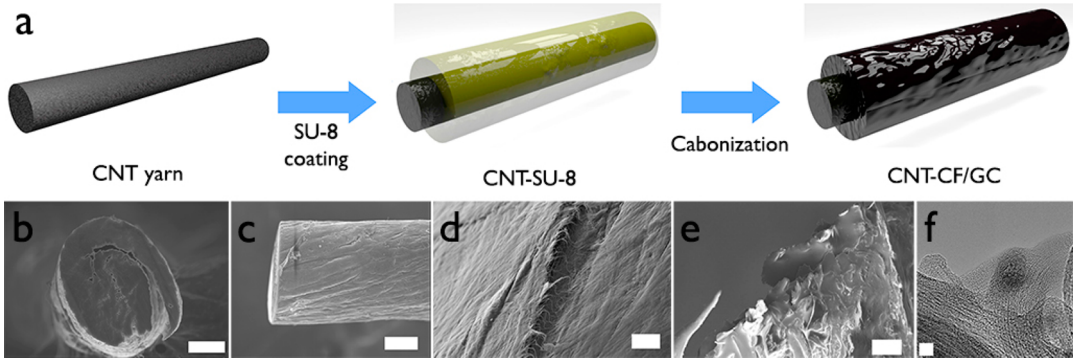

Figure 1. Key process for the fabrication of a CNT yarn−CF/GC core−shell-like hybrid fiber. (a) Schematic of CNT yarn, SU-8 photoresist on the surface of the CNT yarn, and schematic drawing of the CNT yarn−CF/GC hybrid wire after carbonization of SU-8. (b) Cross-sectional SEM of as-spun CNT yarn after cutting using FIB (Forced Ion Beam); the scale bar is 20 μm. (c) Side view of as-spun CNT yarn; the scale bar is 20 μm. (d) High-magnified SEM of the surface of CNT yarn; the scale bar is 200 nm. (e) SEM of cured SU-8 photoresist on the surface of the CNT yarn; the scale bar is 20 μm. (f) High-resolution TEM of CNT yarn; the scale bar is 5 nm. TEM verifies that the CNT yarn is made up of SWCNTs and DWCNTs.

fiber and glassy carbon (CF/GC) core−shell structure with not only dramatically increased thermal and mechanical properties but also the ability to overcome the lower electrical conductivity of CF/GC without any chemical doping and additional processes. CF is used extensively in industries such as aerospace, automobile, and the military, due to its exceptionally high mechanical strength, light weight, high chemical stability, and high thermal conductivity.[32] Conversely, CF has higher electrical resistance than CNTs because in CFs the sheets of carbon atoms are somewhat randomly folded or crumpled together rather than pristinely flat.[33] The synergistic combination of CNTs and CF/GC overcomes their physical deficiencies to create an overall better fiber.

This CNT yarn−CF/GC hybrid is based on a CNT yarn core combined with a multistep coating and curing process to create the surrounding CF/GC shell (see detailed procedure in Methods). Figure 1a shows the key process schematics of the fabrication of the CNT yarn−CF/GC core−shell hybrid material. CNT yarn was spun with a mixture of single-walled CNTs (SWCNTs) and double-walled CNTs (DWCNTs) (Figure 1f and see transmission electron microscope (TEM) images in Figure S1) synthesized using the floating catalyst chemical vapor deposition technique.[21,34] After purification of the as-grown CNTs, they were spun to macroscaled yarn by the wet spinning method as shown in Figure 1b, and c and discussed in previous reports.[35] The cross-sectional SEM (Figure 1b) shows inhomogeneity (voids) of as-spun CNT yarn originating from the spinning process. The carbonization process used to achieve formation of a mixture of CF and GC on the surface of the CNT yarn involved using SU-8 photoresist as the carbon precursor due to the excellent adhesive abilities of its epoxy groups, the extreme stability in the cross-links of cured SU-8 photoresist, the low carbonization temperature (600 °C), and the isometric shrinkage during the carbonization process.[36] Thermal treatments were then performed to carbonize the cured SU-8 photoresist on the CNT yarn core. As a result, the CNT yarn−CF/GC hybrid was successfully fabricated as schematically depicted in Figure 1a.

RESULTS AND DISCUSSION

To elucidate the structure of the CNT yarn−CF/GC system, scanning electron microscopy (SEM) and Raman spectroscopy were conducted, as shown in Figure 2. SEM indicates well-fabricated CF/GC on the surface of the CNT yarn (Figure 2a). Figure 2a clearly shows that the CNT yarn core is completely covered with CF/GC (diameter of hybrid ~170 μm, diameter of CNTs yarn 30−70 μm, thickness of CF/GC 50−80 μm). Figure 2b shows more obviously the unique hybrid system consisting of CNT yarn and CF/GC. The cross-sectional image indicates that the SU-8 carbonization process covered up voids in the CNT yarn formed *via* wet spinning, as shown in Figure 2d. Figure 2e shows the interface between CNT and CF/GC after the ion-milling process. It is clearly seen that CF/GC has a more robust structure than CNTs. After the SU-8 coating and carbonization process, the CNTs have been well-preserved and are without damage (Figure 2c). High-resolution TEM shows the interface between the CNT and CF/GC in Figure 2f. It can be shown that SU-8 was transformed into graphitic carbon fiber and glassy carbon. The Raman spectrum recorded from the surface of the fiber (Figure 2g) has a D band (1355 cm^{-1}) and a G band (1585 cm^{-1}), indicating the breakdown of lattice symmetry with the A_{1g} vibrational mode of the graphite plane and single graphite crystals with the E_{2g} vibrational mode of the graphite cell, respectively.[37] This is a strong indicator of the presence of graphitic structure in the outer shell. The spectrum is preferably close to graphitic carbon.[38−40] Therefore, the outer shell of the fiber is made up of carbon fiber and glassy carbon because the carbonization temperature is not enough to carbonize, completely. Figure 2h exhibits the three XRD spectra recorded from three different samples: carbonized SU-8 at 1000 °C (green) as-grown CNTs (blue) and

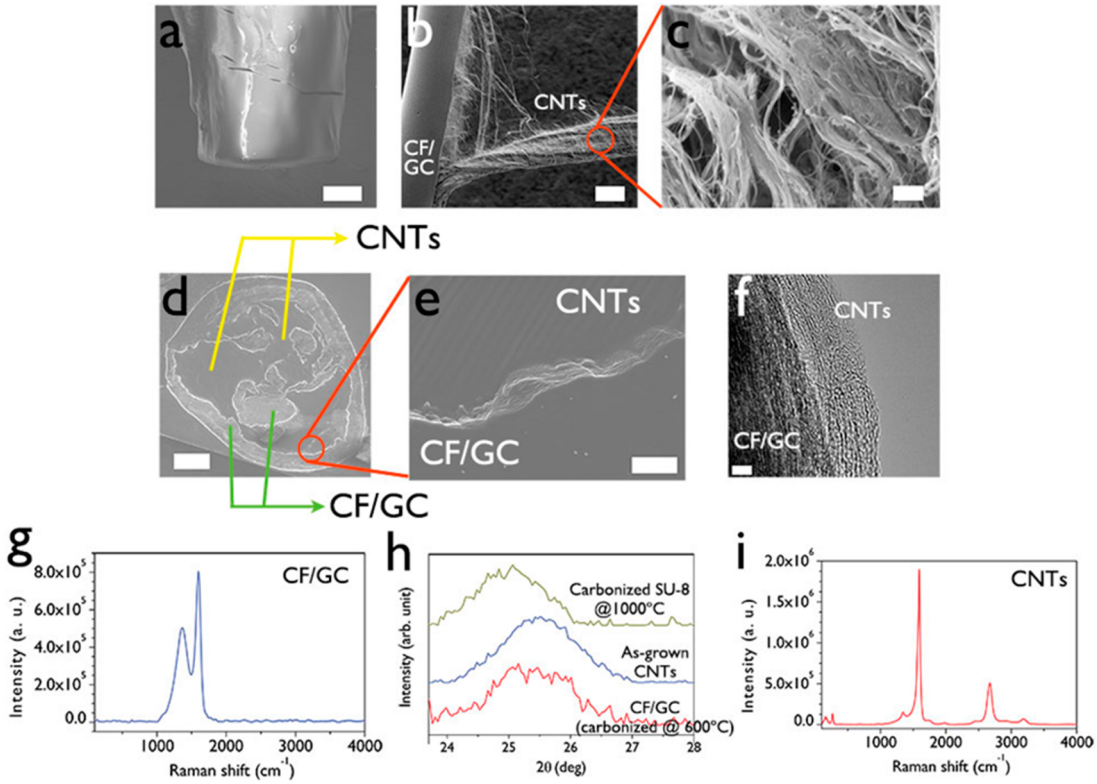

Figure 2. (a) SEM image of the CNT yarn−CF/GC hybrid fiber after carbonization of the SU-8 photoresist; the scale bar is 20 μm. (b) SEM image of the CNT yarn−CF/GC hybrid fiber; the scale bar is 20 μm. (c) SEM image of CNTs in the hybrid fiber; the scale bar is 200 nm. (d) Cross-sectional SEM image of the CNT yarn−CF/GC hybrid fiber after cutting using the ion-milling process; the scale bar is 30 μm. The image indicates that the SU-8 carbonization process covered up voids of the CNT yarn that were formed *via* the spinning process. (e) High-magnification SEM image of the interface between the CNT and CF/GC; the scale bar is 4 μm. (f) High-resolution TEM image of the interface between the CNT and CF/GC; the scale bar is 5 nm. (g) Raman spectrum from the surface of the CF/GC in the outer shell of the CNT yarn−CF/GC hybrid fiber depicting the D band (1335 cm^{-1}) and G band (1585 cm^{-1}). (h) XRD spectra of carbonized SU-8 at 1000 °C, as-synthesized CNT, and CNT yarn−CF/GC. (i) Raman spectrum of the CNT yarn of the hybrid fiber illustrating the RBM, D band (1344 cm^{-1}), and G band (1592 cm^{-1}) of the CNT yarn.

the CNT yarn−CF/GC hybrid (carbonized at 600 °C, red). Typically, graphite has 2θ = 26.603° (d = 0.335 nm) for the (002) diffraction position. The heat treatment (carbonization) at low temperature transforms SU-8 from an epoxy-based negative photoresist to a semicrystalline state. The up-shifted XRD peak for carbonized SU-8 at 1000 °C is at 25.186° and for the CNT yarn-CF/GC at 25.800°. The interlayer spacing d_{002} of each sample is 0.3533 and 0.3450 nm, respectively. The XRD spectral lines intimate that the CNT yarn−CF/GC hybrid has a better graphitic nature than carbonized SU-8 at 1000 °C.[41] The Raman spectrum of the CNT yarn (Figure 2i) has a radial breathing mode (RBM), a D band, a G band, and their overtones.[42] The RBM, strong evidence of the presence of SWCNTs and DWCNTs, verifies that the CNT yarn is composed of SWCNTs and DWCNTs (see peak fitting of RBM in the Supporting Information). A low peak area ratio of the D and G bands (area of D band/area of G band, A_D/A_G, = 0.08) indicates the CNT yarn is made up of very high quality CNTs (low degree of disorder).

The current−voltage (I−V) characteristics of the bare CNT yarn and the CNT yarn−CF/GC hybrid are measured to quantify the electromechanically coupled response. In Figure 3a, the I−V curves of as-spun CNT yarn and the CNT yarn−CF/GC hybrid show that the response of the CNT yarn−CF/GC hybrid is nonlinear and less than the CNT yarn for the entire voltage range (±1.0 V). The electrical resistance, extracted from reciprocal I−V curves, of the CNT yarn−CF/GC hybrid (6.2×10^{-5} Ωm) is an order of magnitude higher than that of the CNT yarn alone (7.9×10^{-6} Ωm). These results imply that CF/GC contributes to the lowering of the electrical conductivity of the hybrid structure due to its relatively high electrical resistance compared to CNT yarn. Despite the increased electrical resistance of the CNT yarn−CF/GC hybrid, its electrical properties are comparable to previously reported CNT yarns and fibers (Table 1).[26]

A self-heating 3ω technique was utilized to measure the thermal conductivities of the CNT yarn−CF/GC hybrid and bare CNT yarn.[43,44] The 3ω signal correlates to the thermal conductivity through eq 1,

$$V_{3\omega,\,\mathrm{rms}} = \frac{4I^3RR'L}{\pi^4 kS} \qquad (1)$$

where L, R, and S are the distance, electrical resistance, and cross-sectional area of the sample, respectively.

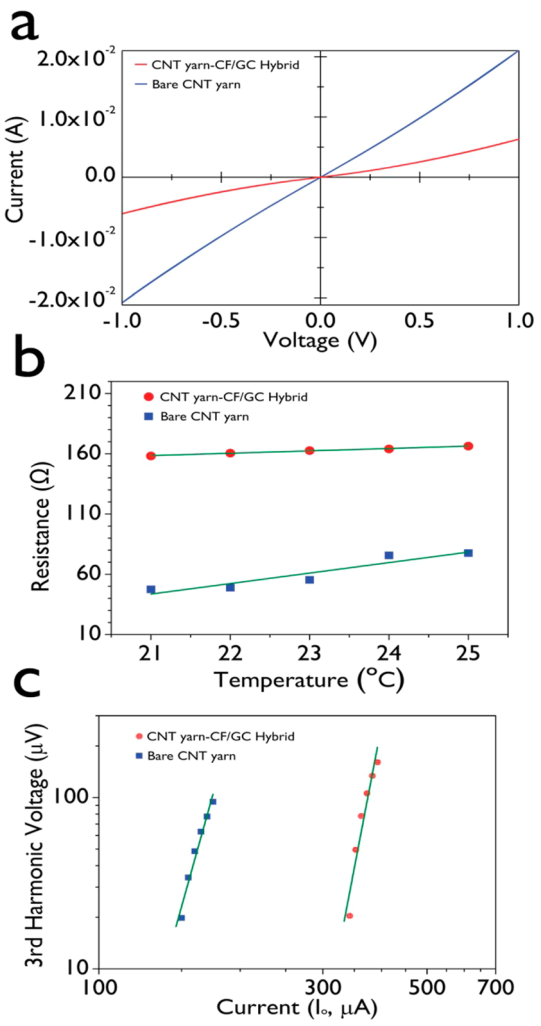

Figure 3. Electrical and thermal characterization of the CNT yarn−CF/GC hybrid fiber and bare CNT yarn. (a) Current−voltage ($I-V$) curves for the CNT yarn−CF hybrid fiber (red) and bare CNT yarn (blue). The electrical resistance, extracted from the reciprocal of the $I-V$ slope, is 6.2×10^{-5} Ωm for the CNT yarn−CF/GC hybrid fiber and 7.9×10^{-6} Ωm for the bare CNT yarn. (b) Resistance at the temperature range 21−25 °C for the CNT yarn−CF hybrid (●) and the bare CNT yarn (■). The temperature coefficients (R') obtained from the slope of the fitted line are 1.97 and 8.7 Ω/°C for the CNT yarn−CF/GC hybrid and the bare CNT yarn, respectively. (c) Third harmonic voltage as a function of input current for the CNT yarn−CF/GC hybrid (●) and the bare CNT yarn (■). Thermal conductivities, calculated from eq 1, are 20.7 W/mK for the CNT yarn−CF hybrid and 64.1 W/mK for the bare CNT yarn.

$R' = (\delta R/\delta T)$ is the temperature gradient of the resistance at the chosen temperature, and k is the thermal conductivity.[45,46] For obtaining the thermal conductivity based on eq 1, the temperature coefficient of the resistance needs to be estimated. The temperature coefficient can be measured from the slope of the linear dependency between the resistances and temperature of the CNT yarn−CF/GC hybrid and bare CNT yarn. Here, we collected the data in the temperature range 21−25 °C, which is close to the measurement temperature of the 3ω signal. As shown in Figure 3b, the measured resistances and temperature coefficients

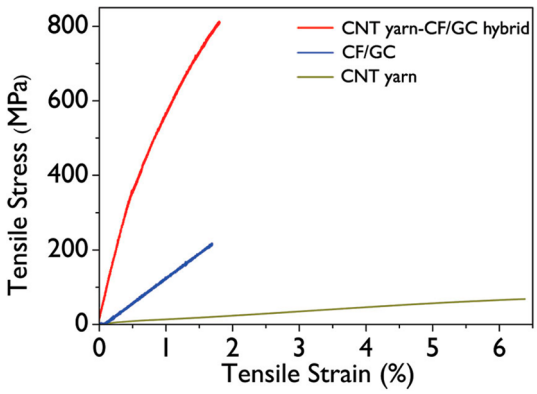

Figure 4. (a) Mechanical tensile stress−strain curves for the CNT yarn−CF/GC hybrid fiber (red), CF/GC (blue), and bare CNT yarn (green). The tensile test was performed at room temperature with a strain rate of 1 μm/min. Tensile strains to failure are 1.7%, 1.6%, and 6.3% for the CNT yarn−CF/GC hybrid fiber, CF/GC, and bare CNT yarn, respectively.

are 49.5 Ω and 8.7 Ω/°C for the CNT yarn and 178.5 Ω and 1.97 Ω/°C for the CNT yarn−CF/GC hybrid. The third-harmonic voltage measurement data were measured at a frequency of 100 Hz. The 3ω signals start appearing at 150 μA for bare CNT yarn and 342 μA for the CNT yarn−CF/GC hybrid wire (Figure 3c). The thermal conductivities calculated with eq 1 were obtained to be 20.7 and 64.1 W/mK for as-spun CNT yarn and the CNT yarn−CF/GC hybrid, respectively. We suspect several mechanisms for the lower thermal conductivity of the bare CNT yarn: tube−tube junctions, intertubular scattering of phonons, and Umklapp scattering (anharmonic scattering).[44] On the other hand, in the case of the CNT yarn−CF hybrid, defect scattering remains dominant over Umklapp scattering.[47]

To demonstrate improved tensile strength of the CNT yarn−CF/GC hybrid, tensile testing was performed (Instron Electopulse) using a strain rate of 1 μm/min. Figure 4 shows the stress−strain curves, measured tensile strengths, and Young's modulus (Table 1) for bare CNT yarn, CF/GC (CF/GC was fabricated without CNT core by carbonization of SU-8), and the CNT yarn−CF/GC hybrid. The wide disparity between the theoretical tensile strength of a single CNT and our experimental value of CNT yarn (68.17 MPa) originates in disorder within the CNT and inhomogeneity generated from the spinning process (Figure 1e). Shown in Figure 4, the CNT yarn−CF hybrid wire has over 11 times higher tensile strength (807 MPa) than bare CNTs (68 MPa) and 4 times higher than CF/GC (210 MPa). The Young's modulus of the hybrid wire is also significantly increased 5 times compared to CF/GC and 4000 times compared to CNT yarn (Table 1).

A possible strengthening mechanism is stress graphitization at the interface between the CNT yarn core and CF/GC. This indicates that the strong interaction between the CNT yarn and CF/GC is generatesd from effective graphitization during carbonization of the

TABLE 1. Comparative Summary of Physical Characteristics with Best Records

	Young's modulus (GPa)	tensile strength (GPa)	electrical resistivity (mΩ · cm)	thermal conductivity (W/mK)
CNT yarn (present study)	0.018	0.068	0.79	20.7
CNT yarn— CF/GC hybrid fiber (present study)	70	0.800	6.2	64.1
CNT yarn	263[a]	3.3[a]	0.015[b]	635[c]
carbon fiber	290[d]	5.65[d]	60[e]	1380[f]

[a] Twisted CNT fiber spun by using hand-held spindle.[51] [b] Iodine-doped SWCNT yarn.[35] [c] Iodine-doped CNT yarn.[52] [d] Commercialized carbon fiber, Amoco T-40.[49] [e] Commercialized carbon fiber, Mitsubishi K637. In the case of carbon fiber heat-treated at 3000 °C, resistivity is 0.66 mΩ · cm.[49] [f] Benzene-derived fiber (BDF) heat-treated at 3000 °C.[53]

SU-8 photoresist. Basically, the CNT yarn has inhomogeneity and torsional stress originating from the spinning process as shown in previous work.[35] The interfacial energy between the CNT yarn core and the cured SU-8 photoresist was also generated during the curing process of SU-8. Moreover, the interfacial energy is also generated as temperature is increased for carbonization by the different thermal expansion of CNT and SU-8. These accumulated stresses on the interface between the core and outer shell can work as driving forces for local graphitization of SU-8 even at a low temperature (600 °C).[48] This is the direct result of the stresses on the interface induced by thermally activated crystallization during graphitization. As a consequence, carbonized SU-8 on the surface of CNT yarn can have a better graphitic nature in spite of carbonization at low temperature. This is in agreement with the results of XRD characterization. The stress graphitization under low-temperature carbonization enables the reinforced tensile strength of the CNT yarn—CF/GC hybrid fiber.

CONCLUSIONS

In summary, a unique hybrid CNT yarn—CF/GC core—shell fiber has been successfully created using a facile multistep process (coating SU-8 photoresist on CNT yarn and low-temperature carbonization). The higher electrical conductivity of the CNT yarn remedies the shortcomings of CF/GC and the better properties of the CF/GC make up for the lower thermal and mechanical properties of the CNT yarn *via* hybridization. The stress graphitization enhances the mechanical properties of the CNT yarn—CF/GC hybrid fiber compared to as-produced CNT yarn and CF/GC. This synergistic combination within the hybrid fiber can be a strong potential for applications of the hybrid fibers. All the physical properties of the hybrid fiber are comparable to the previously reported characteristics of CNT yarns and fibers, shown in Table 1.[35,46,49–53] The hybrid core—shell fiber still has somewhat lower tensile strength and electrical and thermal conductivity than the best records. However, even under low carbonization temperature, the harmonious combination of CNT yarn and CF/GC compensates for their own drawbacks *via* hybridization without any chemical doping and additional processes. Further studies to tailor the physical properties—electrical conductivity and mechanical strength—should be conducted to create high-performance, multifunctional carbon fibers of the future.

METHODS

Creating CNT Yarn. SWCNTs and DWCNTs were grown using the flow chemical vapor deposition (CVD) method. To dissociate the catalysts and remove the amorphous carbon on the CNTs, a purification process was undertaken using oxidation (air conditions at 400 °C for 1 h) and a two-time soaking process (in a 30% hydrogen peroxide solution for 72 h and in a 37% hydrogen chloride solution for another 24 h). Subsequently, the CNT samples were rinsed with DI water until neutralized. By soaking the purified CNT bundle in 98% sulfuric acid for 24 h, the bundle loosens and spreads into a thin film, enabling a small amount of CNT, in ribbon form, to be peeled off from the thin film. A pulling force was applied to the two ends of the ribbon to overcome the tension forces of the sulfuric acid as the CNT ribbon is taken out of the sulfuric acid solution. The ribbon was then dipped into DI water to expel the residual acid and left to dry, causing the ribbon to shrink and become denser as the water evaporated.

Fabrication of CNT Yarn—CF/GC Hybrid. CNT yarn was completely immersed in a solution of negative photoresist (SU-8 2015, Microchem) diluted with cyclopentanone (22% weight ratio) and pulled out at a speed of 1 mm/s. The SU-8-coated CNT yarn was prebaked at 75 °C for 5 min in an oven to remove the solvent, exposed to a 365 nm UV lamp (21 mW/cm^2, Cole-Parmer) for 2 min, and then baked in an oven at 75 °C for 2 min to cross-link the SU-8. To obtain the desired thickness, this coating process was repeated twice under the same conditions. The coated CNT yarn was heated in air to 350 °C at a ramping rate of 5 °C/min, held for an hour to stabilize the coated SU-8, and then cooled. Next, the stabilized sample was heated to 600 °C in high vacuum (order of 10^{-6} Torr) at a ramping rate of 5 °C/min and held for an hour before cooling.

Characterization of Electrical and Thermal Conductivities. The four-point probe third-harmonic method was utilized to eliminate the contact resistance and avoid the spurious signals it causes. A lock-in amplifier (Standford Research System SR850) was used to obtain the 3ω signals by amplifying the small voltage and removing the noise, and an ac current source (Keithley 6221) was used to provide a stable current supply. All the measurements including resistance, temperature, and 3ω signals were done under high vacuum ($p < 10^{-5}$ Torr) in a Janis Research ST-500 cryogenic probe station to reduce radial heat losses through gas conversion.

Mechanical Testing. Tensile mechanical testing was performed using an Instron ElectroPulse E3000 equipped with a 5 kN load cell (ISO11566:1996). The gage length of the fiber samples for the tensile test was 80 mm. All tests were carried out at room temperature and at a strain rate of 1 μm/min. The diameters of the fibers were measured at the fractured ends using SEM after testing. Young's moduli were taken as the slope of a line fitted to

the initial linear regime of the stress–strain curves. The diameters measured by SEM for the CNT yarn–CF/GC hybrid, CF/GC (CF/GC was fabricated without a CNT core by carbonization of SU-8), and bare CNT yarn were *ca.* 25, 35, and 75 μm, respectively.

Conflict of Interest: The authors declare no competing financial interest.

Supporting Information Available: Additional figures. This material is available free of charge *via* the Internet at http://pubs.acs.org.

Acknowledgment. M.G.H., R.V., and P.M.A. acknowledge financial support from the U.S. Army Research Laboratory/Army Research Office (No. W911NF). M.G.H., C.D.P., and P.M.A. acknowledge the support from Exotic Nanocarbons, Japan Regional Innovation Strategy Program by Excellence, JST. P.M.A. and R.V. acknowledge support from the National Science Foundation through grant OISE-0968405. T.N.N., R.V., and P.M.A. acknowledge funding sponsorship from the U.S. Department of Defense, U.S. Air Force Office of Scientific Research, for the Project MURI "Synthesis and Characterization of 3-D Carbon Nanotube Solid Networks" award no. FA9550-12-1-0035. D.P.H. is grateful to the NSF for the Graduate Research Fellowship award grant no. 0940902. J.N. is grateful for the support from Basic Science Research Program through the National Research Foundation of Korea (NRF) funded by the Ministry of Science, ICT & Future Planning (NRF-2013R1A1A1004986). Y.J.J. acknowledges the financial support from Fundamental R&D Program for Core Technology of Materials in the Ministry of Knowledge Economy, Republic of Korea. Y.A.K. acknowledges support from grant no. 24310088 from the Ministry of Education, Culture, Sports, Science and Technology, Japan. B.C.K. acknowledges support from the KIST Institutional Program and the financial support from Fundamental R&D Program for Core Technology of Materials in the Ministry of Knowledge Economy, Republic of Korea.

REFERENCES AND NOTES

1. Kavitha, D.; Priyadarshini, M. A Case Study on Advancements and Applications of Nanotechnology. *Int. J. Adv. Res. Elec. Commun. Eng.* **2013**, *2*, 032–035.
2. Nulle, C.; Miller, C.; Porter, A.; Gandhi, H. *Applications of Nanotechnology to the Brain and Central Nervous System*; Springer: The Netherlands, 2013; Vol. 3, pp 21–41.
3. Tutak, W.; Reynaud, S.; Patel, R. B. Carbon Nanotubes and Their Application to Nanotechnology. In *Bio-Nanotechnology*; Blackwell Publishing Ltd., 2013; pp 464–475.
4. Zobair Ullah, D. Nanotechnology and Its Impact on Modern Computer. *Global J. Res. Eng.* **2013**, *12*, 34–37.
5. Che, G.; Lakshmi, B. B.; Fisher, E. R.; Martin, C. R. Carbon Nanotubule Membranes for Electrochemical Energy Storage and Production. *Nature* **1998**, *393*, 346–349.
6. Zhang, M.; Fang, S.; Zakhidov, A. A.; Lee, S. B.; Aliev, A. E.; Williams, C. D.; Atkinson, K. R.; Baughman, R. H. Strong, Transparent, Multifunctional, Carbon Nanotube Sheets. *Science* **2005**, *309*, 1215–1219.
7. Jung, Y. J.; Kar, S.; Talapatra, S.; Soldano, C.; Viswanathan, G.; Li, X.; Yao, Z.; Ou, F. S.; Avadhanula, A.; Vajtai, R.; *et al.* Aligned Carbon Nanotube–Polymer Hybrid Architectures for Diverse Flexible Electronic Applications. *Nano Lett.* **2006**, *6*, 413–418.
8. Franklin, A. D.; Luisier, M.; Han, S.-J.; Tulevski, G.; Breslin, C. M.; Gignac, L.; Lundstrom, M. S.; Haensch, W. Sub-10 nm Carbon Nanotube Transistor. *Nano Lett.* **2012**, *12*, 758–762.
9. Hahm, M. G.; Leela Mohana Reddy, A.; Cole, D. P.; Rivera, M.; Vento, J. A.; Nam, J.; Jung, H. Y.; Kim, Y. L.; Narayanan, N. T.; Hashim, D. P.; *et al.* Carbon Nanotube–Nanocup Hybrid Structures for High Power Supercapacitor Applications. *Nano Lett.* **2012**, *12*, 5616–5621.
10. Dresselhaus, M. S.; Dresselhaus, G.; Avouris, P. *Carbon Nanotubes: Synthesis, Structure, Properties, and Applications*; Springer-Verlag GmbH: Berlin, 2001.
11. Hone, J.; Whitney, M.; Piskoti, C.; Zettl, A. Thermal Conductivity of Single-Walled Carbon Nanotubes. *Phys. Rev. B* **1999**, *59*, R2514–R2516.
12. Kong, J.; Franklin, N. R.; Zhou, C.; Chapline, M. G.; Peng, S.; Cho, K.; Dai, H. Nanotube Molecular Wires as Chemical Sensors. *Science* **2000**, *287*, 622–625.
13. Srivastava, A.; Srivastava, O.; Talapatra, S.; Vajtai, R.; Ajayan, P. M. Carbon Nanotube Filters. *Nat. Mater.* **2004**, *3*, 610–614.
14. Kocabas, C.; Hur, S.-H.; Gaur, A.; Meitl, M. A.; Shim, M.; Rogers, J. A. Guided Growth of Large-Scale, Horizontally Aligned Arrays of Single-Walled Carbon Nanotubes and Their Use in Thin-Film Transistors. *Small* **2005**, *1*, 1110–1116.
15. Stampfer, C.; Jungen, A.; Linderman, R.; Obergfell, D.; Roth, S.; Hierold, C. Nano-Electromechanical Displacement Sensing Based on Single-Walled Carbon Nanotubes. *Nano Lett.* **2006**, *6*, 1449–1453.
16. Avouris, P.; Chen, Z.; Perebeinos, V. Carbon-Based Electronics. *Nat. Nanotechnol.* **2007**, *2*, 605–615.
17. Itkis, M. E.; Borondics, F.; Yu, A.; Haddon, R. C. Thermal Conductivity Measurements of Semitransparent Single-Walled Carbon Nanotube Films by a Bolometric Technique. *Nano Lett.* **2007**, *7*, 900–904.
18. Li, B.; Hahm, M. G.; Kim, Y. L.; Jung, H. Y.; Kar, S.; Jung, Y. J. Highly Organized Two- and Three-Dimensional Single-Walled Carbon Nanotube–Polymer Hybrid Architectures. *ACS Nano* **2011**, *5*, 4826–4834.
19. Yamada, T.; Hayamizu, Y.; Yamamoto, Y.; Yomogida, Y.; Izadi-Najafabadi, A.; Futaba, D. N.; Hata, K. A Stretchable Carbon Nanotube Strain Sensor for Human-Motion Detection. *Nat. Nanotechnol.* **2011**, *6*, 296–301.
20. Vigolo, B.; Pénicaud, A.; Coulon, C.; Sauder, C.; Pailler, R.; Journet, C.; Bernier, P.; Poulin, P. Macroscopic Fibers and Ribbons of Oriented Carbon Nanotubes. *Science* **2000**, *290*, 1331–1334.
21. Ci, L.; Rao, Z.; Zhou, Z.; Tang, D.; Yan, X.; Liang, Y.; Liu, D.; Yuan, H.; Zhou, W.; Wang, G.; *et al.* Double Wall Carbon Nanotubes Promoted by Sulfur in a Floating Iron Catalyst CVD System. *Chem. Phy. Lett.* **2002**, *359*, 63–67.
22. Ericson, L. M.; Fan, H.; Peng, H.; Davis, V. A.; Zhou, W.; Sulpizio, J.; Wang, Y.; Booker, R.; Vavro, J.; Guthy, C.; *et al.* Macroscopic, Neat, Single-Walled Carbon Nanotube Fibers. *Science* **2004**, *305*, 1447–1450.
23. Li, Y.-L.; Kinloch, I. A.; Windle, A. H. Direct Spinning of Carbon Nanotube Fibers from Chemical Vapor Deposition Synthesis. *Science* **2004**, *304*, 276–278.
24. Zhang, M.; Atkinson, K. R.; Baughman, R. H. Multifunctional Carbon Nanotube Yarns by Downsizing an Ancient Technology. *Science* **2004**, *306*, 1358–1361.
25. Ci, L.; Punbusayakul, N.; Wei, J.; Vajtai, R.; Talapatra, S.; Ajayan, P. M. Multifunctional Macroarchitectures of Double-Walled Carbon Nanotube Fibers. *Adv. Mater.* **2007**, *19*, 1719–1723.
26. Behabtu, N.; Green, M. J.; Pasquali, M. Carbon Nanotube-Based Neat Fibers. *Nano Today* **2008**, *3*, 24–34.
27. Zhang, X.; Jiang, K.; Feng, C.; Liu, P.; Zhang, L.; Kong, J.; Zhang, T.; Li, Q.; Fan, S. Spinning and Processing Continuous Yarns from 4-Inch Wafer Scale Super-Aligned Carbon Nanotube Arrays. *Adv. Mater.* **2006**, *18*, 1505–1510.
28. Koziol, K.; Vilatela, J.; Moisala, A.; Motta, M.; Cunniff, P.; Sennett, M.; Windle, A. High-Performance Carbon Nanotube Fiber. *Science* **2007**, *318*, 1892–1895.
29. Ma, W.; Liu, L.; Zhang, Z.; Yang, R.; Liu, G.; Zhang, T.; An, X.; Yi, X.; Ren, Y.; Niu, Z.; *et al.* High-Strength Composite Fibers: Realizing True Potential of Carbon Nanotubes in Polymer Matrix through Continuous Reticulate Architecture and Molecular Level Couplings. *Nano Lett.* **2009**, *9*, 2855–2861.
30. Ryu, S.; Lee, Y.; Hwang, J.-W.; Hong, S.; Kim, C.; Park, T. G.; Lee, H.; Hong, S. H. High-Strength Carbon Nanotube Fibers Fabricated by Infiltration and Curing of Mussel-Inspired Catecholamine Polymer. *Adv. Mater.* **2011**, *23*, 1971–1975.
31. Liu, Y.; Kumar, S. Recent Progress in Fabrication, Structure, and Properties of Carbon Fibers. *Pol. Rev.* **2012**, *52*, 234–258.
32. Minus, M.; Kumar, S. The Processing, Properties, and Structure of Carbon Fibers. *Publ. Min. Met. Mater. Soc.* **2005**, *57*, 52–58.

33. Dresselhaus, M. S.; Dresselhaus, G.; Sugihara, K.; Spain, I. L.; Goldberg, H. A. *Graphite Fibers and Filaments*; Springer-Verlag: Berlin, 1988; Vol. 5.
34. Wei, J.; Ci, L.; Jiang, B.; Li, Y.; Zhang, X.; Zhu, H.; Xu, C.; Wu, D. Preparation of Highly Pure Double-Walled Carbon Nanotubes. *J. Mater. Chem.* **2003**, *13*, 1340–1344.
35. Zhao, Y.; Wei, J.; Vajtai, R.; Ajayan, P. M.; Barrera, E. V. Iodine Doped Carbon Nanotube Cables Exceeding Specific Electrical Conductivity of Metals. *Sci. Rep.* **2011**, *1*, 83.
36. Park, B. Y.; Taherabadi, L.; Wang, C.; Zoval, J.; Madou, M. J. Electrical Properties and Shrinkage of Carbonized Photoresist Films and the Implications for Carbon Microelectromechanical Systems Devices in Conductive Media. *J. Electrochem. Soc.* **2005**, *152*, J136–J143.
37. Tuinstra, F.; Koenig, J. L. Raman Spectrum of Graphite. *J. Chem. Phys.* **1970**, *53*, 1126–1130.
38. Chu, P. K.; Li, L. Characterization of Amorphous and Nanocrystalline Carbon Films. *Mater. Chem. Phys.* **2006**, *96*, 253–277.
39. Ferrari, A. C.; Robertson, J. Interpretation of Raman Spectra of Disordered and Amorphous Carbon. *Phys. Rev. B* **2000**, *61*, 14095–14107.
40. Tai, F. C.; Wei, C.; Chang, S. H.; Chen, W. S. Raman and X-ray Diffraction Analysis on Unburned Carbon Powder Refined from Fly Ash. *J. Raman Spectrosc.* **2010**, *41*, 933–937.
41. Sharma, S.; Sharma, A.; Cho, Y.-K.; Madou, M. Increased Graphitization in Electrospun Single Suspended Carbon Nanowires Integrated with Carbon-MEMS and Carbon-NEMS Platforms. *ACS Appl. Mater. Interfaces* **2012**, *4*, 34–39.
42. Dresselhaus, M. S.; Eklund, P. C. Phonons in Carbon Nanotubes. *Adv. Phys.* **2000**, *49*, 705–814.
43. Choi, T. Y.; Poulikakos, D.; Tharian, J.; Sennhauser, U. Measurement of Thermal Conductivity of Individual Multiwalled Carbon Nanotubes by the 3-ω Method. *Appl. Phys. Lett.* **2005**, *87*, 013108–3.
44. Choi, T.-Y.; Poulikakos, D.; Tharian, J.; Sennhauser, U. Measurement of the Thermal Conductivity of Individual Carbon Nanotubes by the Four-Point Three-ω Method. *Nano Lett.* **2006**, *6*, 1589–1593.
45. Cahill, D. G.; Pohl, R. O. Thermal Conductivity of Amorphous Solids above the Plateau. *Phys. Rev. B* **1987**, *35*, 4067–4073.
46. Aliev, A. E.; Guthy, C.; Zhang, M.; Fang, S.; Zakhidov, A. A.; Fischer, J. E.; Baughman, R. H. Thermal Transport in MWCNT Sheets and Yarns. *Carbon* **2007**, *45*, 2880–2888.
47. Heremans, J.; Beetz, C. P., Jr. Thermal Conductivity and Thermopower of Vapor-Grown Graphite Fibers. *Phys. Rev. B* **1985**, *32*, 1981–1986.
48. Lanticse-Diaz, L. J.; Tanabe, Y.; Enami, T.; Nakamura, K.; Endo, M.; Yasuda, E. The Effect of Nanotube Alignment on Stress Graphitization of Carbon/Carbon Nanotube Composites. *Carbon* **2009**, *47*, 974–980.
49. Donnet, J.-B. *Carbon Fibers*, 3rd ed.; CRC Press LLC, 1998.
50. Morgan, P. *Carbon Fibers and Their Composites*; Taylor & Francis: Boca Raton, FL, 2005; Vol. 1.
51. Zhang, X.; Li, Q.; Holesinger, T. G.; Arendt, P. N.; Huang, J.; Kirven, P. D.; Clapp, T. G.; DePaula, R. F.; Liao, X.; Zhao, Y.; *et al*. Ultrastrong, Stiff, and Lightweight Carbon-Nanotube Fibers. *Adv. Mater.* **2007**, *19*, 4198–4201.
52. Behabtu, N.; Young, C. C.; Tsentalovich, D. E.; Kleinerman, O.; Wang, X.; Ma, A. W. K.; Bengio, E. A.; ter Waarbeek, R. F.; de Jong, J.; Hoogerwerf, R. E.; *et al*. Strong, Light, Multifunctional Fibers of Carbon Nanotubes with Ultrahigh Conductivity. *Science* **2013**, *339*, 182–186.
53. Nysten, B.; Piraux, L.; Issi, J. P. Thermal Conductivity of Pitch-Derived Fibres. *J. Phys. D: Appl. Phys.* **1985**, *18*, 1307.